pH Imaging

A Review of pH Measurement Methods and Applications in Cancers

BY ROBERT J. GILLIES, NATARAJAN RAGHUNAND, MARIA L. GARCIA-MARTIN, AND ROBERT A. GATENBY

In mammalian tissues, intra- and extracellular pH are regulated in a dynamic steady state driven by metabolic acid production, export of H^+ from cells, and diffusion of these H^+ equivalents from the site of production to the blood, where they are buffered by an open and dynamic CO_2/HCO_3^- system. Although this balance is quite robust, it can be altered in many pathological states, notably cancers, renal failure, ischemia, or chronic obstructive pulmonary disease. Current methods to assess acid-base balance in patients are limited to systemic monitoring (e.g., blood gasses, urine pH, etc.) and cannot assess regiospecific imbalances that may occur. In recent years, noninvasive measures of tissue pH have been developed that can assess the intra- and/or extracellular pH of tissues. These are primarily *magnetic resonance* (MR) based, and their spatiotemporal resolution has continuously improved. MR-based methods are on the horizon to measure intra- or extracellular pH with imaging (ca. 0.1 mm) resolution in vivo. Although this article primarily focuses on the measurement of pH in cancers, the applicability of these methods to other pathologies will also be discussed.

Regulation of Tissue pH

The end-products of energy metabolism are invariably acids. This is true whether metabolism ends with anaerobically produced lactic acid, or aerobically produced CO_2, which is hydrated to form carbonic acid that dissociates into bicarbonate plus a free proton (Figure 1). The carbons in these compounds originate from sugars, amino acids, or lipids. Sugars, such as glucose, are transported into cells via specific permease transporters, such as the GLUT1-GLUT12 family of glucose transporters (System 2 in Figure 1). Once inside the cell, sugars are metabolized to pyruvate. In the absence of oxygen, this is reduced to lactate in order to recycle the NADH that is required at an earlier step in glycolysis. This anaerobically produced lactate is exported from cells via the monocarboxylate transporter, illustrated as System 4 in Figure 1 [1]–[3]. The proton, H^+, is produced during oxidation of glyceraldehyde phosphate and contributes to cytosolic acidification. Lowering of intracellular pH stimulates the export of protons via a number of carrier systems (System 3 in Figure 1) including Na^+/H^+ exchange (NHE) [4]–[6], vacuolar H^+ ATPases [7]–[9] and Na^+-dependent HCO_3^- exchangers [10]–[13]. While NHE is commonly accepted as the major proton exporting system in mammalian cells, all three systems are present and perform overlapping functions. Hence, there is some redundancy in this system and activities of these transporters can substitute for one another in the presence of inhibitors. Table 1 lists the proton exporting systems observed in mammalian cells. All cells express NHE and anion exchange activities to varying degrees, and both have been implicated in altered pH regulation [4], [14]. Vacuolar-type ATPases are thought to exert their effects through the export and recycling of acidic vesicles to the cell surface [15], and this activity is not universally seen. In addition to these, carbonic anhydrases also participate in pH regulation, either through providing HCO_3^- to anion exchange or by the net transport of protons [16]. Figure 2 shows an activity plot for NHE as a function of intracellular pH under basal and serum-stimulated conditions. This illustrates that the activity of NHE is regulated by the intracellular pH, thus, the pHi is highly regulated to reach a "set point." Hence, alterations in intracellular pH are not caused by metabolic overload but, instead, are highly regulated by the activities of proton exporting systems.

In the presence of oxygen, pyruvate can be oxidized by mitochondria ("M" in Figure 1) to CO_2. Similarly, in many obligatorily aerobic organs, e.g., cardiac muscle, free fatty acids or ketone bodies (FFA/KB), are oxidized by mitochondria to CO_2. FFA are carried in the blood associated with albumins. Most cells have fatty acids stored as tri-acyl glycerol microdomains, which can be observed in ^{1}H-MRS [17], [18]. The FFA can be released through activation of cyclic AMP-dependent lipases. FFA and KB are free to diffuse across the plasma membrane on demand, provided to cells via specific carrier proteins [19], [20]. The CO_2 is produced oxidatively by the Krebs cycle. Although it can cross the membrane rapidly, its transport rate is greatly facilitated by water channels, or aquaporins [21]. Once outside the cell, CO_2 is hydrated by carbonic anhydrases (I–XII) to form bicarbonate plus a proton. Proton production rates are on the order of 1–20 nmol min^{-1} mg $protein^{-1}$. "Free" protons do not exist in tissues. Instead, they are in equilibrium bound to buffers species. Diffusion of H^+-equivalents from the site of production to the blood occurs in associate with mobile buffers, such as phosphate and bicarbonate [22], [23]. This occurs on a

 0739-5175/04/$20.00©2004IEEE

background of immobile buffers, primarily histidines in proteins, and sulfates in glycoseaminoglycans. These immobile buffers, as well as phosphate in bone, play a major role in maintaining acid-base balance, especially in response to ingested acids or alkali. Passive buffering capacity is limited, hence, active physiologic responses are also required to maintain the acid-base balance at the cell and tissue level. These physiologic processes can be at the cellular level, such as through feedback changes in metabolism, and at the systemic level, involving adaptive changes to the excretion of volatile acids by the lungs and fixed acids by the kidneys [24]. Bicarbonate accounts for about 86% of extracellular buffering, but only about 36% of intracellular buffering, with nonbicarbonate buffers (proteins, inorganic phosphate) making up the rest [25], [26].

Why Measure pH?

Alterations in acid-base homeostasis are common in pathology. For example, tumor interstitial fluid has a reduced buffering capacity compared to normal tissue and this, in combination with poor perfusion and increased lactic acid secretion by tumors [27], is believed to result in an acidic extracellular pH (pHe) in tumors [28]. This situation is exacerbated by the lowered buffering capacity of bicarbonate, the primary extracellular buffer, at more acidic pH. This acidic pHe in tumors has a significant number of important consequences, listed in Table 2. From this list, it can be seen that low pH plays a role in tumor initiation, progression, and therapy.

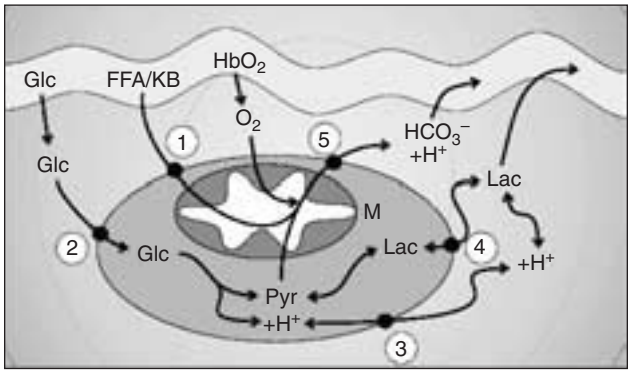

Fig. 1. Acid-producing metabolism. Blood supplies glucose (Glc), free fatty acids and keytone bodies (FFA/KB), and oxygen on hemoglobin (HbO_2), which diffuse to target cells within 0.2 mm of capillaries. Glc is transported into cells via hexose-specific permeases (System 2) where it is oxidized to pyruvate (Pyr) and a proton (H^+) via glycolysis. The H+ is exported from the cell via a number of transporters (System 3), iterated in Table 1. In the absence of oxygen, Pyr is reduced to lactate (Lac), which is transported out of the cell via monocarboxylate transporters (MCT, System 4) whereupon it enters the blood via passive diffusion. In the presence of oxygen, Pyr is oxidized to CO_2, whose exit from the cell is facilitated by aquaporins (system 5), whereupon it is hydrated by carbonic anhydrases to HCO_3^- and an H^+. FFAs and KBs enter cells (System 1) and are also oxidized to CO_2 in the presence of oxygen. The extracellular protons diffuse into the blood in association with mobile buffers, such as HCO_3^- and phosphate.

Table 1. Proton-equivalent transporters in mammalian cells.

Family	Human Isoforms	Inhibitors
Na/H exchange	NHE1-NHE3	amilorides
HCO_3 transport	AE1-5 (electroneutral) NBC1-4 (electrogenic)	stilbenes
Vacuolar-ATPases	13+ subunits with variable expression	bafilomycins, concanamycins
Carbonic Anhydrases	CA I- CA XII	acetazolimides
H^+/K^+ ATPases	Renal, Stomach	omeprazoles

Pathologically altered renal or pulmonary physiology can also manifest with perturbations in systemic and renal pH. The generation of 50–100 mEq/day of acid in the typical adult diet is normally excreted by the resorbtion of filtered HCO_3^- in the proximal tubule and the secretion of H^+ in the distal tubule. In the clinical setting there are three general mechanisms that lead to metabolic acidosis: addition or overproduction of acid, failure of normal renal acid secretion, and loss of bicarbonate or alkaline equivalents [29]. Renal tubular metabolic acidosis (RTA) syndromes can involve the proximal tubule (Type 2) or the distal tubule (Types 1 and 4). Impaired proximal tubule acidification may result from a defect in the apical Na^+/H^+ antiporter, the basolateral Na^+/HCO_3^- symporter, the apical H^+-ATPase, or the intracellular or luminal isoforms of carbonic anhydrase [30]. Distal RTA can be due to defective proton pumps (H^+-ATPase or H^+-K^+-ATPase) [7], [31] or defects in Cl^-/HCO_3^- exchange [32]. The renal tubular H^+-ATPase is regulated by aldosterone, and aldosterone deficiency (or resistance) can also cause distal RTA [33]. Chronic obstructive pulmonary disease (COPD) is a common ailment and results in lower lung tidal volumes, retention of CO_2, and, hence, chronic respiratory acidosis. The effects of chronic systemic acidosis on disease progression and etiopathology are not well understood.

Measurements of In Vivo pH with ^{31}P MRS

Several techniques have been proposed for the measurement of tissue pH by MR spectroscopy (MRS) and MRI. Some of these techniques exploit endogenous MR resonances while others require the administration of exogenous agents. Tissue pH, particularly in tumors, can be estimated from the ^{31}P MR resonance of inorganic phosphate (P_i) [27]. Because intracellular P_i concentrations are 2–3 mM, compared to ca. 1.0 mM for extracellular, and because the intracellular volume fractions are generally greater than 50%, the chemical shift of the endogenous Pi resonance is generally assumed to reflect *intracellular* pH. However, in some pathological states, such as necrosis, the extracellular Pi can also be visible, giving rise to a complex set of resonances [34]. The pH-sensitive ^{31}P MR resonance of 3-aminopropylphosphate (3-APP) has been used by us and others to measure extracellular pH of tumors in mice [35]. This compound is nontoxic, membrane impermeant, and has a chemical shift dependence of ca. 1 ppm pH unit^{-1}. Figure 3(a) is a ^{31}P spectrum of an MCF-7 tumor in a mouse injected with 3-APP, illustrating the phosphonate resonances downfield of the endogenous phosphates. Figure 3(b) shows the effect of bicarbonate on the chemical shift of 3-APP, indicating tumor alkalinization and Figure 3(c) shows the structure of 3-APP, highlight-

ing the ionizable hydroxyl group. It has been used by a number of groups who have consistently observed that the pHe is lower than the pHi in tumor xenografts, whereas this "gradient" is reversed in normal tissues (Table 3).

Measurements of In Vivo pH with ^{19}F MRS

Molecules with pH-sensitive ^{19}F resonances have also been developed. The spin 1/2 resonance of ^{19}F has advantages in that it has a high gyromagnetic ratio, relatively large chemical shift dispersion, and an almost total lack of endogenous resonances in normal tissues. Hence, resonances from exogenous agents are readily resolved. Drawbacks of ^{19}F approaches can include instability of fluorinated compounds and the inability to measure simultaneously other metabolic compounds. These drawbacks are being addressed with improved halogenation chemistries and the development of double tuned ^{19}F-^{1}H probes and electronics. Early during development of this approach, Deutsch and Taylor developed a series of fluorinated alanines that distributed across cell membranes and yielded pH-sensitive resonances [36]–[39]. However, this approach was limited to perfused cells and was not applied in vivo. Mason and his coworkers have developed a fluorinated derivative of vitamin B6, 6-fluoropyridoxol, which readily enters cells. They have measured both the intracellular and extracellular pH in rodent tumors by resolving the pH-sensitive ^{19}F resonance arising from the two compartments [40]. They have recently shown that the triflouromethylated derivative of pyridoxal is membrane impermeant and insensitive to temperature, with a pKa of 6.82 [41]. Griffith's group has investigated the application of the extracellular ^{19}F pH probe ZK-150471 [34], [42]. The performance of this probe was systematically compared to ^{31}P MRS of 3-APP and was found to have superior signal-to-noise and resolvable pH-dependent chemical shifts. Both 3-APP and ZK-150471 are cell-impermeant and report only the extracellular pH, although ^{31}P MRS of 3-APP offers the possibility of simultaneous measurement of intracellular pH from the P_i resonance.

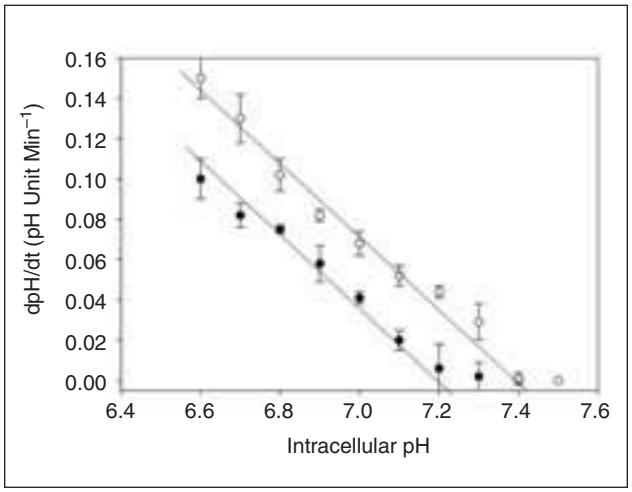

Fig. 2. Set-point of Na/H exchange, NHE. The recovery rate of intracellular pH from an ammonium induced acid load is measured using intracellularly-loaded fluorescent dyes, such as SNARF-1(70) and is converted to a scalar rate (nmole H^+ min^{-1} mg $protein^{-1}$ after correction for the intracellular passive buffering capacity, β. Results show recovery rates as a function of pHi for NIH-3T3 fibroblasts under basal unstimulated conditions (●) and following stimulation with epidermal growth factor, EGF (O).

Table 2. Consequences of tumor acidity (69).

- Spontaneous transformation
- Radio resistance
- Hyperthermic sensitization
- Ion trapping of weak base drugs
- Increased in vivo metastasis
- Increased invasion
- Increased mutation rate
- Increased chromosomal rearrangements
- Altered gene expression

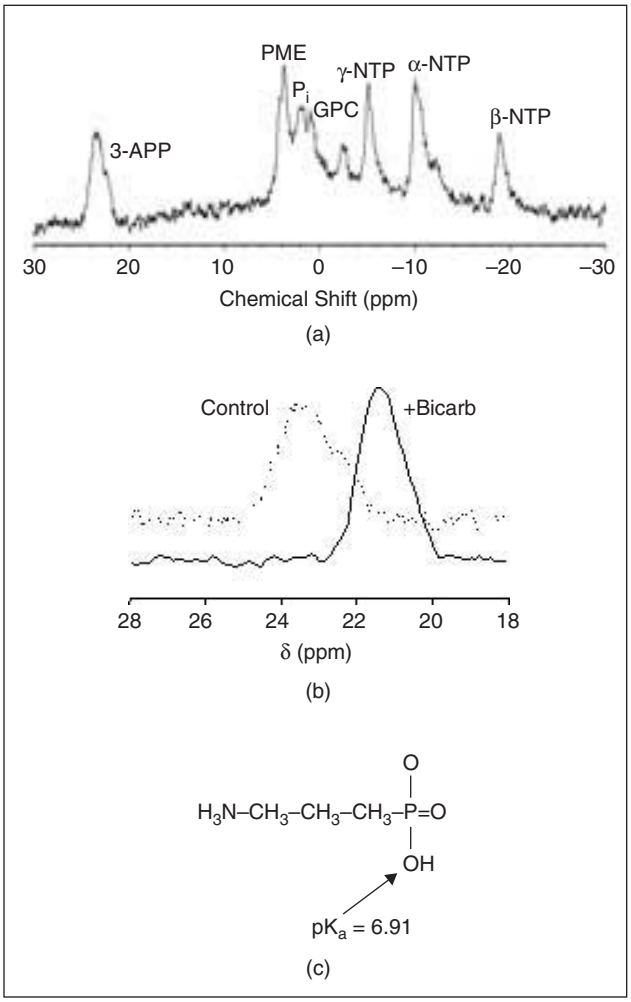

Fig. 3. ^{31}P MRS Measurement of pH. Mice bearing MCF-7 tumor xenografts were injected with 3-APP (c) and ^{31}P spectra acquired 30–50 min later (a). Intra- and Extracellular pH values can be estimated from the chemical shifts of inorganic phosphate, Pi, and 3-APP, respectively. (b) illustrates the effect of acute oral bicarbonate on the chemical shift of 3-APP, indicating an alkaline shift of tumor pHe.

Table 3. Intra- and extracellular pH of tumors measured with ^{31}P MRS (69).

Tumor	Species	Type	Extracellular pH $(pHe)_{ex}$	Intracellular pH (pHi)
C3h	Mouse	Breast c.	6.95 ± 0.18	7.19 ± 0.11
RIF-1	Mouse	Fibrosarcoma	6.87 ± 0.03	7.02 ± 0.01
Ehrlich	Mouse	Breast c.	6.69 ± 0.05	6.92 ± 0.05
CaNT	Mouse	Adenocarcinoma	6.70 ± 0.05	7.08 ± 0.06
9618a	Rat	Hepatoma	6.70 ± 0.03	7.12 ± 0.02
Walker	Rat	Sarcoma	6.30 ± 0.04	7.04 ± 0.04
MNU-induced	Rat	Breast	6.80 ± 0.07	7.16 ± 0.07
Normal	Rat	Liver	7.34 ± 0.03	7.26 ± 0.02
Normal	Rat	Muscle	7.39	7.39 ± 0.10
MCF-7	Human	Breast c.	6.99 ± 0.11	7.15 ± 0.08
MDAmb-435	Human	Breast c.	6.80 ± 0.11	7.37 ± 0.07
HT-29	Human	Colon Ado	6.79 ± 0.05	7.02 ± 0.05

Measurements of In Vivo pH with ^{1}H MRS

The ^{1}H nucleus offers the highest inherent sensitivity, and it is possible to image the spatial distribution of tissue pH in vivo by the use of probes with pH-sensitive ^{1}H resonances. We and others have employed an exogenously administered imidazole, IEPA, developed by Cerdan, Ballesteros, and colleagues [43], [44]. This compound has a pH-dependent chemical shift of the H-2 resonance in the 7–9 ppm range, is nontoxic, and membrane-impermeant (Figure 4). This has been used for imaging pHe in orthotopic breast cancer [45], [46] and brain tumors [47] in rodents by MR spectroscopic imaging (MRSI). An advantage of this approach is that this downfield region of the in vivo ^{1}H MR has few interfering background resonances. In fact, endogenous aromatic imidazoles like histidine also have pH-sensitive ^{1}H resonances in this region of the spectrum, but most of these species occur at concentrations that are too low to exploit. Vermathen et al. [48] have overcome this problem by orally loading human subjects with histidine and have been able to measure brain pH a few hours later by localized ^{1}H MRS. MRS and MRSI approaches are generally dependent on measuring the pH-dependent chemical shifts. Hence, such measurements are theoretically independent of the concentration of the pH probe. However, the spatial resolution is limited to 1–2 mm, which is lower spatially than other techniques based on imaging. This is illustrated in Figure 5, which shows a 2-mm slice from an MDA-mb-435 breast cancer tumor in a severe combined immunodeficient (SCID) mouse. The right side of this illustration is the pHe map generated from MRSI of the IEPA resonance, which was followed by a dynamic contrast enhancement series using Omniscan [46]. A drawback to this approach is the relatively insensitivity of chemical shift to pH, since there is only ca. 0.7 ppm shift over the entire titration range. While this may be appropriate for higher field studies, it likely precludes the use of this approach on clinical scanners at 1.5 T.

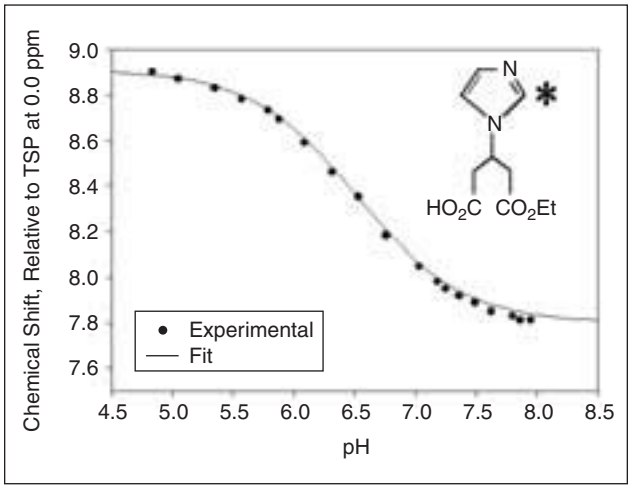

Fig. 4. pH-dependent chemical shift of IEPA. The chemical shift of the H2 of (±) 2-imidazole-1-yl-3-ethoxycarbonyl-propionic acid, IEPA (*, inset), is pH-dependent, as shown here with in vitro titration.

pH Imaging with Magnetization Transfer

Water in biological systems exists as bulk phase H_2O and in association with the macromolecules and metabolites that make up tissues. Associated, or "bound," water generally has a shortened T2, hence, is not visible in a typical MR experiment. However, these two states of water are in dynamic equilibrium, hence, irradiation, or saturation, of the magnetization of the bound water can be transferred to the bulk phase. This is the basis of the conventional magnetization transfer (MT) effect, first described for imaging by Balaban and Ward [49]. Water interacts with macromolecules and solutes through either dipolar coupling, e.g., through hydrogen bonds, or through chemical exchange, wherein the hydrogens of water exchange with hydrogens on ionizable groups, $X \sim H$. All such exchanges will be acid or base-catalyzed and thus have pH dependence. The majority of magnetization transfer from macromolecules to bulk water is most likely due to dipolar coupling and not

In recent years, noninvasive measures have been developed that can assess the intra- and/or extracellular pH of tissues.

chemical exchange [50], although contrary viewpoints exist [51], [52]. However, there are particularities of chemical exchange dependent effects that allow it to be selectively interrogated [53]. This is the case when the exchangeable resonances can be distinguished in MR spectra, i.e., those in slow exchange on the MR time scale. This is not the case for the solid-like structures causing the conventional MT effect, but it is the case for exchangeable amide protons in small mobile peptides and proteins in the tissue [52]. Specifically, chemical exchange saturation transfer (CEST) can be distinguished from dipolar coupling in that CEST is inherently pH dependent and occurs at specific frequencies that are asymmetric with respect to the water resonance, whereas dipolar coupling manifests primarily as a shortening of T2 and, thus, is symmetric about the water resonance.

In an MT experiment, irradiation of the sample at the exact frequency of the bound hydrogen will reduce the net magnetic moment of those spins during their bound lifetimes. This reduction in magnetization (saturation) is transferred to bulk water as the hydrogens exchange. Saturation-transfer phenomena have been described for decades (e.g., [54]) and the formalism for such processes is well developed [55], [56]. For chemical exchange processes, the reduction in bulk water signal intensity depends on the T_1, the exchange rate constants (k_{on} and k_{off}) and the concentrations of each species [52], [57]:

$$\mathrm{PTR} = \frac{k}{R_{1w}}\frac{[H_x]}{[H_w]}\left(1 - e^{-R_{1w}t_{sat}}\right),$$

where PTR is the proton transfer rate, k is the normalized first-order rate constant for exchange, R_{1w} is the relaxation rate for water protons, t_{sat} is the saturation time and $[H_x]$ and $[H_w]$ are the concentrations of carrier and water hydrogens, respectively. Hydrogens bound to carrier groups resonate at frequencies different from that of bulk water by an amount, $+\Delta\omega$. If $+\Delta\omega$ is small, irradiation will also generate a direct saturation of the water resonance in dipolar exchange. However, this direct saturation is symmetric, whereas the carrier-bound hydrogen resonances are asymmetrically displaced with respect to water. Consequently, saturation irradiation at $+\Delta\omega$ will provide a signal that is distinct from that at $-\Delta\omega$. With high B_1 and B_0 homogeneity, the difference between signals (images) obtained at $+\Delta\omega$ and $-\Delta\omega$ will be sensitive to CEST effects, and pH dependence can be empirically determined.

CEST approaches can be applied using exchange of hydrogens with ionizable groups that are either endogenous or exogenous. In all cases, CEST effects have to be separated from conventional MT effects, which are approximately (but not completely) symmetric. Endogenous groups can include the amide hydrogens of proteins that resonate downfield of water [58]. The region of the ^{1}H MR spectrum around 8.3 ppm contains several very low and undetectable resonances from N-bound protons, which are in fast exchange with solvent water. This fast exchange with water protons renders these resonances problematic to detect with pulse sequences which employ water presaturation. Zijl and his colleagues have devised a pulse sequence to permit visualization of these resonances, and have demonstrated that it is possible to measure pH from the pH-sensitive rate of exchange with water protons of one or more of these protons [57]. Figure 6 shows a resulting pH map that can be calculated using the asymmetric amide proton exchange in mouse brain following regional

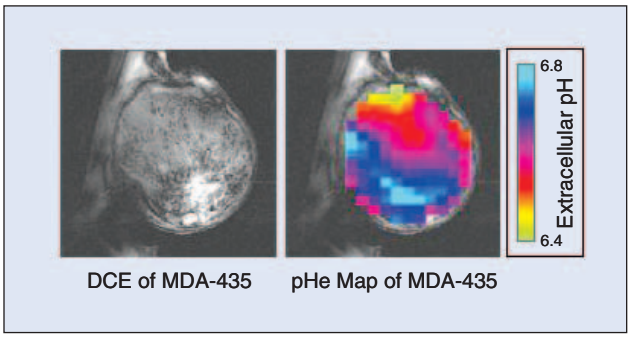

Fig. 5. pHe maps from IEPA. IEPA was injected i.p. into SCID mice bearing MDA-mb-435 tumors and the pHe was estimated from the chemical shift of H-2 using magnetic resonance spectroscopic imaging, MRSI. Following this, perfusion was estimated using dynamic contrast enhancement in response to bolus i.v. injection of Gd(DOTA).

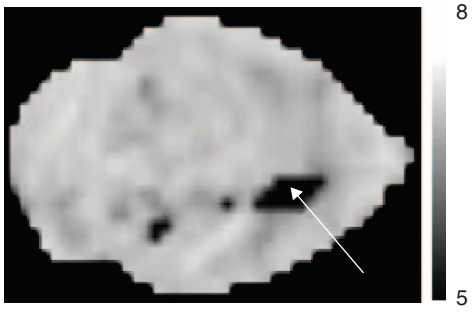

Fig. 6. pH image from amide proton exchange. The asymmetry of magnetization transfer at ± 3–4 ppm centered about the water resonance can be used to calculate the amide proton exchange rate, which is pH dependent. This has been used to generate pH maps in rodent brain following regional ischemia, indicated by the arrow (57). (Courtesy of PCM van Zijl).

The end-products of energy metabolism are invariably acids.

ischemia. Similar work has also been performed in experimental gliomas [59].

On the other hand, more specific CEST effects can be obtained with exogenous agents. Ward and Balaban [49] demonstrated that the use of a compound such as 5,6-dihydrouracil with multiple proton exchange sites each with different pH dependencies allows for the possibility of a "ratiometric" calculation of solution pH which would be independent of variations in water proton T_1 times and the concentrations of sites exchanging protons with water. The use of polypeptide gene-carriers for such pH studies has also been proposed [60]. A disadvantage of these techniques is the need to inject large amounts of the pH-sensitive agent in order to be able to image pH with acceptable sensitivity and spatial resolution. A possible solution to the large concentration requirement has been proposed independently by Aime and Sherry, who have synthesized Europium-containing pH-dependent chelates that imparts large (> +50 ppm) contact shifts on water protons [61], [62]. The magnitude of this chemical shift imparts a greater MT effect and significantly reduces the direct saturation of the bulk water resonance. These effects are typically shown in a *z*-plot, which plots the magnitude of the bulk water resonance as a function of the frequency of saturation. A challenge to the development of these agents is the optimization of the exchange rate. Too fast an exchange rate makes it more difficult to fully saturate the bound spins within energy deposition (SAR) limits. If spins are not fully saturated, the effects are nonsteady state and more difficult to quantify. However, too slow an exchange rate will significantly reduce the CEST effect. A strength of these MT approaches is the internal control of acquiring an image without saturation, yielding direct and robust quantification of effect. However, as below, the quantification is critically dependent on knowing the concentration of contrast reagent.

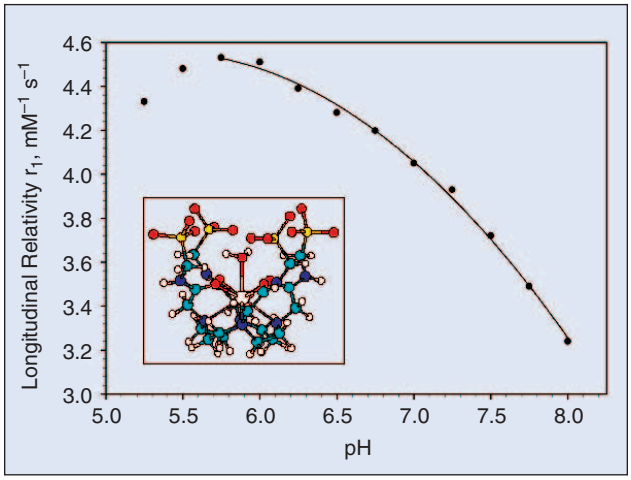

Fig. 7. Titration of the water-proton longitudinal relaxivity of GdDOTA-4AmP in phosphate-buffered saline at 37°C, 4.7 T (67). (Inset) Hyperchem™ structure of GdDOTA-4AmP. (Courtesy of A. Dean Sherry.)

pH-Dependent Relaxation Agents

Recent years have seen the development of gadolinium-based contrast agents whose relaxivity is dependent on pH [63]–[65]. Like CEST, these agents provide the possibility of imaging pH with spatial resolution comparable to that of standard MRI. As in CEST, the magnitude of the effect is dependent on the local concentration of contrast reagent (CR), as well as the pH. Hence, accurate methods must be developed with which to determine the spatial- and time-variant CR concentrations, in order to convert the observed relaxivity to a molar relaxivity and thus, pH. Figure 7 shows the structure of Gd(DOTA)-4AmP^{5-}, which contains four ionizable phosphonate groups that catalyze the pH-dependent hydrogen exchange to the Gd-bound water, as well as the pH-dependent molar relaxivity [63]. This compound is nontoxic and membrane-impermeant and distributes with pharmacokinetics similar to that of the identically charged, but pH-independent, Gd(DOTP)$^{5-}$. Hence, one approach to uniquely compute a pH using such agents is by sequential administration of Gd(DOTP)$^{5-}$ and Gd(DOTA)-4AmP^{5-}, calculating the time- and spatially variant concentrations of Gd(DOTP)$^{5-}$ from T1-weighted images and then using these values to correct for the time- and spatially variant concentrations of Gd(DOTP)$^{5-}$ [66]. Such an approach has been successfully applied to the measurement of renal pH [67], [68]. Kidneys provide good systems to develop these methods as the pharmacokinetics of these agents are rapid and reproducible. Also, as most of the extracellular fluid in the kidney is tubular, the calculated values can be validated with measurements of urine pH. With their leaky vasculature and slower washout, however, tumors have less favorable pharmacokinetics and present a greater challenge. Despite these challenges, the dual injection protocol has been successfully applied to small brain tumors [Garcia-Martin, in preparation]. Although the dual-injection protocol may be appropriate for imaging of pH in animal models, it will be difficult to perform such an operation in the clinic. Hence, there is a need to develop methods that can simultaneously measure relaxation and concentration in a single injection.

Summary

Acid-base balance is altered in a variety of common pathologies, including COPD, ischemia, renal failure, and cancer. Because of robust cellular pH homeostatic mechanisms, most of the pathological alterations in pH are expressed as changes

in the extracellular, systemic pH. There are data to indicate that altered pH is not simply an epiphenomenon of metabolic or physiologic imbalance but that chronic pH alterations can have important sequelae.

MRSI and MRI measurements indicate that pH gradients of up to 1.0 pH unit can exit within 1-cm distance. Although measurement of blood pH can indicate systemic problems, it cannot pinpoint the lesion or quantitatively assess the magnitude of excursion from normal pHe. Hence, there is a need to develop pHe measurement methods with high spatiotemporal resolution. The two major approaches being investigated include magnetization transfer methods and relaxation methods. pH-dependent MT effects can observed with endogenous signals or exogenously applied CEST agents. While endogenous signals have the advantage of being fully noninvasive and relatively straightforward to apply, they lack a full biophysical characterization and dynamic range that might be afforded by future CEST agents. pH-dependent relaxivity also requires the injection or infusion of exogenous contrast reagents. In both MT and relaxographic approaches, the magnitude of the effect, and, thus, the ability to quantify pHe, depends on a spatially and temporally varying concentration of the CR. A number of approaches have been proposed to solve this problem and, once it is solved, pH imaging methods will be applicable to human clinical pathologies.

Acknowledgments

The authors would like to thank Dr. Peter van Zijl, Dr. A. Dean Sherry, and Dr. Howard Lien for critical comments and providing figures. This work was supported by NIH grants R01 CA77575 (RJG), R01 CA93650 (RAG), R21 DK63124 (NR), and the Southwest Animal Imaging Resource, SWAIR R24 CA88588.

Robert J. Gillies received his Ph.D. in 1979 from the University of California, Davis. He is a professor of biochemistry and molecular biophysics, physiology, and radiology and the director of the Molecular Imaging Program at the University of Arizona Health Sciences Center.

Natarajan Raghunand is an associate research scientist at the Arizona Cancer Center, University of Arizona. He received his B.Tech. in chemical engineering from the Indian Institute of Technology, Madras, India; his M.S. in chemical engineering from Colorado State University; and his Ph.D. in chemical engineering from Texas A&M University. His research focuses on the influence of the tumor microenvironment on cancer progression and response to therapy and development of contrast-enhanced MRI techniques to image aspects of renal and tumor physiology.

Maria L. Garcia-Martin is a post-doctoral researcher at the Arizona Cancer Center. She received her Ph.D. from the Biomedical Research Institute in Madrid, Spain. Her research primarily focuses on intracellular pH regulation and metabolism as detected by MRI techniques.

Robert A. Gatenby graduated from Princeton University and received his M.D. from the University of Pennsylvania. He completed his residency in diagnostic radiology at the Hospital of the University of Pennsylvania and is currently a professor of radiology and applied mathematics at the University of Arizona. His research interests include mathematical modeling of tumor invasion with a particular emphasis on the role of the tumor microenvironment. He is also interested in the application of information theory and evolutionary game theory to carcinogenesis.

Address for Correspondence: Robert J. Gillies, Dept. Biochemistry, Arizona Cancer Center 1515 N. Campbell Ave., Tucson, AZ 85724-5024 USA. E-mail: rgillies@email.arizona.edu.

References

[1] A. Schurr, R.S. Payne, J.J. Miller, M.T. Tseng, and B.M. Rigor, "Blockade of lactate transport exacerbates delayed neuronal damage in a rat model of cerebral ischemia," *Brain Res.*, vol. 895, no. 1–2, pp. 268–272, Mar. 2001.

[2] C. Zhao, M.C. Wilson, F. Schuit, A.P. Halestrap, and G.A. Rutter, "Expression and distribution of lactate/monocarboxylate transporter isoforms in pancreatic islets and the exocrine pancreas," *Diabetes*, vol. 50, no. 2, pp. 361–366, Feb. 2001.

[3] D. Eladari, R. Chambrey, T. Irinopoulou, F. Leviel, F. Pezy, P. Bruneval, M. Paillard, and R.A. Podevin, "Polarized expression of different monocarboxylate transporters in rat medullary thick limbs of Henle," *J. Biol. Chem.*, vol. 274, no. 40, pp. 28420–28426, Oct. 1999.

[4] R.A. Kandasamy, F.H. Yu, R. Harris, A. Boucher, J.W. Hanrahan, and J. Orlowski, "Plasma membrane Na^+/H^+ exchanger isoforms (NHE-1,-2, and -3) are differentially responsive to second messenger agonists of the protein kinase A and C pathways," *J. Biol. Chem.*, vol. 270, no. 49, pp. 29209–29216, Dec. 1995.

[5] R.T. Miller, L. Counillon, G. Pages, R.P. Lifton, C. Sardet, and J. Pouyssegur, "Structure of the 5′-flanking regulatory region and gene for the human growth factor-activatable Na^+/H^+ exchanger NHE-1," *J. Biol. Chem.*, vol. 266, pp. 10,813–10,819, 1991.

[6] C. Sardet, P. Fafournoux, and J. Pouyssegur, "Alpha-thrombin, epidermal growth factor, and okadaic acid activate the Na^+/H^+ exchanger, NHE-1, by phosphorylating a set of common sites," *J. Biol. Chem.*, vol. 266, pp. 19,166–19,171, Oct. 1991.

[7] S. Gluck and J. Caldwell, "Immunoaffinity purification and characerizatin of vacuolar H^+ATPase from bovine kidney," *J. Biol. Chem.*, vol. 262, pp. 15,780–15,789, May 1987.

[8] C.J. Swallow, S. Grinstein, and O.D. Rotstein, "A vacuolar type H^+-ATPase regulates cytoplasmic pH in murine macrophages," *J. Biol. Chem.*, vol. 265, pp. 7645–7654, May 1990.

[9] R. Martinez-Zaguilan, R.M. Lynch, G.M. Martinez, and R.J. Gillies, "Vacuolar type proton ATPases are functionally expressed in the plasma membranes of human tumor cells," *Am. J. Physiol.*, vol. 265, pp. c1015–c1029, Oct. 1993.

[10] R.D. Vaughan-Jones and K.W. Spitzer, "Role of bicarbonate in the regulation of intracellular pH in the mammalian ventricular myocyte," *Biochem. & Cell Biology*, vol. 80, no. 5, pp. 579–596, 2002.

[11] T.L. Pannabecker, O.H. Brokl, Y.K. Kim, D.E. Abbott, and W.H. Dantzler, "Regulation of intracellular pH in rat renal inner medullary thin limbs of Henle's loop," *Pflugers Archiv—European J. Physiol.*, vol. 443, no. 3, pp. 446–457, Jan. 2002.

[12] M.F. Romero, "The electrogenic Na^+/HCO_3^- cotransporter NBC," *JOP. J. Pancreas*, vol. 2, no. 4 (Suppl.), pp. 182–191, 2001.

[13] H. Yamada, S. Yamazaki, N. Moriyama, C. Hara, S. Horita, Y. Enomoto, A. Kudo, H. Kawakami, Y. Tanaka, T. Fujita, and G. Seki, "Localization of NBC-1 variants in human kidney and renal cell carcinoma," *Biochem. Biophys. Res. Comm.*, vol. 310, pp. 1213–1218, Oct. 2003.

[14] M.L. Wahl, P.M. Pooler, P. Briand, D.B. Leeper, and C.S. Owen, "Intracellular pH regulation in a nonmalignant and a derived malignant human breast cell line," *J. Cellular Physiol.*, vol. 183, no. 3, pp. 373–380, June 2000.

[15] R. Martinez-Zaguilan, N. Raghunand, R.M. Lynch, W. Bellamy, G.M. Martinez, B. Rojas, D. Smith, W.S. Dalton, and R.J. Gillies, "pH and drug resistance. I. Functional expression of plasmalemmal V-type H^+-ATPase in drug-resistant human breast carcinoma cell lines," *Biochem. Pharmacol.*, vol. 57, no. 9, pp. 1037–1046, May 1999.

[16] P. Lehenkari, T.A. Hentunen, T. Laitala-Leinonen, J. Tuukkanen, and H.K. Vaananen, "Carbonic anhydrase II plays a major role in osteoclast differentiation and bone resorption by effecting the steady state intracellular pH and $Ca2^+$," *Experimental Cell Res.*, vol. 242, no. 1, pp. 128–137, July 1998.

[17] C. Remy, N. Fouilhe, I. Barba, E. Sam-Lai, H. Lahrech, M.G. Cucurella, M. Izquierdo, A. Moreno, A. Ziegler, R. Massarelli, M. Decorps, and C. Arus, "Evidence that mobile lipids detected in rat brain glioma by 1H nulear magnetic resonance correspond to lipid droplets," *Cancer Res.*, vol. 57, no. 3, pp. 407–414, Feb. 1997.

[18] Y. Perez, H. Lahrech, M.E. Cabanas, R. Barnadas, M. Sabes, C. Remy, and C. Arus, "Measurement by nuclear magnetic resonance diffusion of the dimensions of

the mobile lipid compartment in C6 cells," *Cancer Res.*, vol. 62, no. 20, pp. 5672–5677, Oct. 2002.
[19] B. Binas, X.X. Han, E. Erol, J.J. Luiken, J.F. Glatz, D.J. Dyck, R. Motazavi, P.J. Adihetty, D.A. Hood, and A. Bonen, "A null mutation in H-FABP only partially inhibits skeletal muscle fatty acid metabolism," *Amer. J. Physiol.—Endocrinology and Metabolism*, vol. 285, no. 3, pp. E481–E489, Sept. 2003.
[20] P. Besnard, I. Niot, H. Poirier, L. Clement, and A. Bernard, "New insights into the fatty acid-binding protein (FABP) family in the small intestine," *Molecular and Cell. Biochem.*, vol. 239, no. 1–2, pp. 139–147, Oct. 2002.
[21] M. Endo, R. Jain, B. Witwer, and D. Brown, "Water channel (Aquaporin 1) expression and distribution in mammary carcinomas and glioblastomas," *Microvascular Res.*, vol. 58, pp. 89–98, Sept. 1999.
[22] J.R. Griffiths, D.J. McIntyre, F.A. Howe, and M. Stubbs, "Why are cancers acidic? A carrier-mediated diffusion model for H^+ transport in the interstitial fluid," in *Novartis Foundation Symp.*, vol. 240, 2001, pp. 46–62.
[23] P.A. Schornack and R.J. Gillies, "Contributions of cell metabolism and H^+ diffusion to the acidic pH of tumors," *Neoplasia (New York)*, vol. 5, no. 2, pp. 135–145, 2003.
[24] H.E. Adrogue and H.J. Adrogue, "Acid-base physiology," *Respiratory Care*, vol. 46, no. 4, pp. 328–341, Apr. 2001.
[25] H.J. Adrogue and N.E. Madias, "Management of life-threatening acid-base disorders. First of two parts," *New Eng. J. Med.*, vol. 338, no. 1, pp. 26–34, Jan. 1998.
[26] H.J. Adrogue and N.E. Madias, "Management of life-threatening acid-base disorders. Second of two parts," *New Eng. J. Med.*, vol. 338, no. 2, pp. 107–111, Jan. 1998.
[27] M. Stubbs, Z.M. Bhujwalla, G.M. Tozer, L.M. Rodrigues, R.J. Maxwell, R. Morgan, F.A. Howe, and J.R. Griffiths, "An assessment of 31P MRS as a method of measuring pH in rat tumours," *NMR Biomed.*, vol. 5, no. 6, pp. 351–359, Nov. 1992.
[28] N. Raghunand, M.I. Altbach, R. van Sluis, B. Baggett, C.W. Taylor, Z.M. Bhujwalla, and R.J. Gillies, "Plasmalemmal pH-gradients in drug-sensitive and drug-resistant MCF-7 human breast carcinoma xenografts measured by 31P magnetic resonance spectroscopy," *Biochem. Pharmacology*, vol. 57, no. 3, pp. 309–312, Feb. 1999.
[29] E.R. Swenson, "Metabolic acidosis," *Respiratory Care*, vol. 46, no. 4, pp. 342–353, Apr. 2001.
[30] N.A. Kurtzman, "Renal tubular acidosis syndromes," *Southern Med. J.*, vol. 93, no. 11, pp. 1042–1052, Nov. 2000.
[31] T.L. Caviston, W.G. Campbell, C.S. Wingo, and B.D. Cain, "Molecular identification of the renal H^+, K^+-ATPases," *Seminars Nephrology*, vol. 19, no. 5, pp. 431–437, Sept. 1999.
[32] P. Jarolim, C. Shayakul, D. Prabakaran, L. Jiang, A. Stuart-Tilley, H.L. Rubin, S. Simova, J. Zavadil, J.T. Herrin, J. Brouillette, M.J. Somers, E. Seemanova, C. Brugnara, L.M. Guay-Woodford, and S.L. Alper, "Autosomal dominant distal renal tubular acidosis is associated in three families with heterozygosity for the R589H mutation in the AE1 (band 3) Cl-/HCO3- exchanger," *J. Biol. Chem.*, vol. 273, no. 11, pp. 6380–6388, Mar. 1998.
[33] D.C. Battle, "Hyperkalemic hypercholoremic metabolic acidosis associated with selective aldosterone deficiency and distal renal tubular acidosis," *Seminars Nephrol*, vol. 1, pp. 260–273, 1981.
[34] A.S. Ojugo, P.M. McSheehy, D.J. McIntyre, C. McCoy, M. Stubbs, M.O. Leach, I.R. Judson, and J.R. Griffiths, "Measurement of the extracellular pH of solid tumours in mice by magnetic resonance spectroscopy: A comparison of exogenous (19)F and (31)P probes," *NMR Biomed.*, vol. 12, no. 8, pp. 495–504, Dec. 1999.
[35] R.J. Gillies, Z. Liu, and Z. Bhujwalla, "31P-MRS measurements of extracellular pH of tumors using 3-aminopropylphosphonate," *Amer. J. Physiol.*, vol. 267, no. 1, pt. 1, pp. t-203, July 1994.
[36] C. Deutsch, J.S. Taylor, and D.F. Wilson, "Regulation of intracellular pH by human peripheral blood lymphocytes as measured by 19-F NMR," in *Proc. Nat. Academy of Sciences: USA*, vol. 79, pp. 7944–7948, 1982.
[37] C. Deutsch, J.S. Taylor, and M. Price, "pH Homeostatis in human lymphocytes: Modulation by ions and mitogen," *J. Cell Biol.*, vol. 98, pp. 885–894, Mar. 1984.
[38] J.S. Taylor, C. Deutsch, G.G. McDonald, and D.F. Wilson, "Measurement of Transmembrane pH gradients in human erythrocytes using 19F-NMR1," *Analytical Biochem.*, vol. 114, no. 1, pp. 415–418, 1981.
[39] J.S. Taylor and C. Deutsch, "Fluorinated alpha-methylamino acids as 19-F NMR indicators of intracellular pH," *Biophys. J.*, vol. 43, pp. 261–267, Sept. 1983.
[40] R.P. Mason, "Transmembrane pH gradients in vivo: Measurements using fluorinated vitamin B6 derivatives," *Current Medicinal Chem.*, vol. 6, pp. 481–499, June 1999.
[41] W. Cui, P.Y.J. Otten, V. Kodibagkar, and R.P. Mason, "6-trifluoromethyl pyridoxal, a novel reporter molecule for tumor extracellular pH," in *Proc. Int. Soc. for Magnetic Resonance in Medicine*, 2003, vol. 11, p. 623.
[42] P.M. McSheehy, M.T. Seymour, A.S. Ojugo, L.M. Rodrigues, M.O. Leach, I.R. Judson, and J.R. Griffiths, "A pharmacokinetic and pharmacodynamic study in vivo of human HT29 tumours using 19F and 31P magnetic resonance spectroscopy," *Eur. J. Cancer*, vol. 33, no. 14, pp. 2418–2427, Dec. 1997.
[43] M.S. Gil, F. Cruz, S. Cerdan, and P. Ballesteros, "Imidazol-1-ylalkanoate esters and their corresponding acids. A novel series of extrinsic ^{1}H NMR probes for intracellular pH," *Bioorganic and Med. Chem. Lett.*, vol. 2, no. 12, pp. 1717–1722, 1992.
[44] S. Gil, P. Zaderenzo, F. Cruz, S. Cerdan, and P. Ballesteros, "Imidazol-1-ylalkanoic acids as extrinsic ^{1}H NMR probes for the determination of intracellular pH, extracellular pH and cell volume," *Bioorganic and Med. Chem. Lett.*, vol. 2, no. 5, pp. 305–314, 1994.
[45] R. van Sluis, Z.M. Bhujwalla, N. Raghunand, P. Ballesteros, J. Alvarez, S. Cerdan, J.P. Galons, and R.J. Gillies, "In vivo imaging of extracellular pH using 1H MRSI," *Magnetic Resonance in Med.*, vol. 41, no. 4, pp. 743–750, Apr. 1999.
[46] Z.M. Bhujwalla, D. Artemov, P. Ballesteros, S. Cerdan, R.J. Gillies, and M. Solaiyappan, "Combined vascular and extracellular pH imaging of solid tumors," *NMR Biomed.*, vol. 15, no. 2, pp. 114–119, Apr. 2002.
[47] M.L. Garcia-Martin, G. Herigault, C. Remy, R. Farion, P. Ballesteros, J.A. Coles, S. Cerdan, and A. Ziegler, "Mapping extracellular pH in rat brain gliomas in vivo by 1H magnetic resonance spectroscopic imaging: Comparison with maps of metabolites," *Cancer Res.*, vol. 61, no. 17, pp. 6524–6531, Sept. 2001.
[48] P. Vermathen, A.A. Capizzano, and A.A. Maudsley, "Administration and ^{1}H MRS detection of histidine in human brain: Application to in vivo pH measurement," *Magnetic Resonance Med.*, vol. 43, no. 5, pp. 665–675, May 2000.
[49] K.M. Ward and R.S. Balaban, "Determination of pH using water protons and chemical exchange dependent saturation transfer (CEST)," *Magnetic Resonance Med.*, vol. 44, no. 5, pp. 799–802, Nov. 2000.
[50] R.M. Henkelman, G.J. Stanisz, and S.J. Graham, "Magnetization transfer in MRI: A review," *NMR in Biomed.*, vol. 14, no. 2, pp. 57–64, Apr. 2001.
[51] E. Liepinsh and G. Otting, "Proton exchange rates from amino acid side chains—implications for image contrast," *Magnetic Resonance Med.*, vol. 35, no. 1, pp. 30–42, Jan. 1996.
[52] P.C. van Zijl, J. Zhou, N. Mori, J.F. Payen, D. Wilson, and S. Mori, "Mechanism of magnetization transfer during on-resonance water saturation. A new approach to detect mobile proteins, peptides, and lipids," *Magnetic Resonance Med.*, vol. 49, no. 3, pp. 440–449, Mar. 2003.
[53] W. Kucharczyk, P.M. MacDonald, G.J. Stanisz, and R.M. Henkelman, "Relaxivity and magnetization transfer of white matter lipids at MR imaging: Importance of cerebrosides and pH[1]," *Radiology*, vol. 192, pp. 521–529, Aug. 1994.
[54] S. Forsen and R. Hoffman, "Study of moderately rapid chemical exchange reactions by means of nuclear magnetic double resonance," *J. Chem. Phys.*, vol. 39, pp. 2892–2901, 1963.
[55] D. Leibfritz and W. Dreher, "Magnetization transfer MRS," *NMR Biomed.*, vol. 14, no. 2, pp. 65–76, Apr. 2001.
[56] S.D. Wolff and R.S. Balaban, "Magnetization transfer contrast (MTC) and tissue water proton relaxation in vivo," *Magnetic Resonance Med.*, vol. 10, pp. 135–144, Apr. 1989.
[57] J. Zhou, J.F. Payen, D.A. Wilson, R.J. Traystman, and P.C. van Zijl, "Using the amide proton signals of intracellular proteins and peptides to detect pH effects in MRI," *Nature Med.*, vol. 9, no. 8, pp. 1085–1090, Aug. 2003.
[58] S. Mori, S.M. Eleff, U. Pilatus, N. Mori, and P.C. van Zijl, "Proton NMR spectroscopy of solvent-saturable resonances: A new approach to study pH effects in situ," *Magnetic Resonance Med.*, vol. 40, no. 1, pp. 36–42, July 1998.
[59] J. Zhou, B. Lal, D. Wilson, J. Laterra, and P.C. van Zijl, "Amide proton transfer (APT) contrast for imaging of brain tumors," *Magnetic Resonance Med.*, vol. 50, pp. 1120–1126, Dec. 2003.
[60] P.C. van Zijl, N. Goffeney, J. Duyn, L.H. Bryant, and J. Bulte, "The use of starburst dendrimers as pH contrast agents," in *Proc. Int. Soc. Magnetic Resonance in Med.*, 2003, vol. 9, p. 878.
[61] S. Aime, A. Barge, C.D. Delli, F. Fedeli, A. Mortillaro, F.U. Nielsen, and E. Terreno, "Paramagnetic lanthanide(III) complexes as pH-sensitive chemical exchange saturation transfer (CEST) contrast agents for MRI applications," *Magnetic Resonance Med.*, vol. 47, no. 4, pp. 639–648, Apr. 2002.
[62] S. Zhang, P. Winter, L. Wu, and A.D. Sherry, "A novel Europium(III)-based MRI contrast agent," *J. Amer. Chem. Soc.*, vol. 123, pp. 1517–1518, Feb. 2001.
[63] S. Zhang, K. Wu, and A.D. Sherry, "A novel pH-sensitive MRI contrast agent," *Angewandte Chemie Int. Ed.*, vol. 38, pp. 3192–3194, Dec. 1999.
[64] S. Aime, M. Botta, S.G. Crich, G. Giovenzana, G. Palmisano, and M. Sisti, "Novel paramagnetic macromolecular complexes derived from the linkage of a macrocyclic Gd(III) complex to polyamino acids through a squaric acid moiety," *Biocon. Chem.*, vol. 10, no. 2, pp. 192–199, Mar.-Apr. 1999.
[65] M. Mikawa, M. Miwa, M. Brautigam, T. Akaike, and A. Maruyama, "Gd^{3+} loaded polyion complex for pH depiction with magnetic resonance imaging," *J. Biomed. Mat. Res.*, vol. 49, pp. 390–395, Mar. 2000.
[66] D.A. Beauregard, D. Parker, and K.M. Brindle, "Relaxation-based mapping of tumor pH," in *Proc. Int. Soc. for Magnetic Resonance in Med.*, 1998, vol. 6, p. 53.
[67] N. Raghunand, C. Howison, A.D. Sherry, S. Zhang, and R.J. Gillies, "Renal and systemic pH imaging by contrast-enhanced MRI," *Magnetic Resonance Med.*, vol. 49, no. 2, pp. 249–257, Feb. 2003.
[68] N. Raghunand, S. Zhang, A.D. Sherry, and R.J. Gillies, "In vivo magnetic resonance imaging of tissue pH using a novel pH-sensitive contrast agent, GdDOTA-4AmP," *Academic Radiology*, vol. 9, supp. 2, pp. S481–S483, Aug. 2002.
[69] R.J. Gillies, N. Raghunand, G.S. Karczmar, and Z.M. Bhujwalla, "MRI of the tumor microenvironment," *J. Magnetic Resonance Imaging*, vol. 16, no. 4, pp. 430–450, Oct. 2002.
[70] R. Martinez-Zaguilan, G.M. Martinez, F. Lattanzio, and R.J. Gillies, "Simultaneous measurement of intracellular pH and Ca^{2+} using the fluorescence of SNARF-1 and Fura-2," Amer. J. Physiol., vol. 260, pp. C297–C307, Feb. 1991.